Soft Matter

Observation of a Structural Gradient in Winsor-III Microemulsion Systems

Journal:	*Soft Matter*
Manuscript ID	SM-ART-02-2018-000322.R3
Article Type:	Paper
Date Submitted by the Author:	16-May-2018

Complete List of Authors:	Hayes, Douglas; Dept Biosystems Engineering and Soil Science, Professor Pingali, Sai Venkatesh; Oak Ridge National Laboratory, Biology and Soft Matter Division O'Neill, Hugh; Oak Ridge National Laboratory, Chemical Sciences Division Urban, Volker; Oak Ridge National Laboratory, Biology and Soft Matter Division Ye , Ran; University of Tennessee Knoxville, Department of Food Science and Technology

Observation of a Structural Gradient in Winsor-III Microemulsion Systems

Douglas G. Hayes *[,1], Sai Venkatesh Pingali *[,2], Hugh M. O'Neill [2], Volker S. Urban [2], and Ran Ye [1]

[1] Department of Biosystems Engineering and Soil Science, University of Tennessee, Knoxville, TN 37996-4531 USA, [2]Neutron Sciences Division, Oak Ridge National Laboratory, P.O. Box 2008, Oak Ridge, TN 37831-6475; *To whom all correspondences should be addressed (dhayes1@utk.edu; tel 865-974-7991; fax 865-974-4514; pingalis@ornl.gov; tel 865-241-2424; fax 865-574-6268)

5/16/18

Abstract

We demonstrate here for the first time via small-angle neutron scattering (SANS) that the middle, bicontinuous microemulsion (BμE), phase of Winsor-III systems undergoes gradual change of structure and composition in the vertical direction, contrary to the commonly held belief of uniform structure and composition. A vertical stage was deployed to enable precise alignment of a custom-designed rectangular cell containing the W_{III} system with respect to the neutron beam, allowing for several different vertical positions to be analyzed. For the water/AOT/CK-2,13 (two-tailed alkyl ethoxylate containing a 1,3-dioxolane linkage)/heptane Winsor-III system, the quasi-periodic repeat distance (d) and correlation length (ξ), obtained from the Teubner-Strey model applied to the SANS data, decreased and the surface area per volume of the surfactant monolayer (via Porod analysis) increased in the downward direction, trends that reflect an increase of surfactant concentration, consistent with the ultralow interfacial tension that often occurs for the lower liquid-liquid interface of many W_{III} systems. The water/ sodium dodecyl sulfate (SDS)/1-pentanol/ dodecane system shared the same trend with regard to d as observed for AOT/CK-2,13. In contrast, for SDS/pentanol, ξ increased and the amphiphilicity factor (f_a) decreased in the downward direction, trends consistent with a decrease of cosurfactant (pentanol) concentration in the downward direction. Non-uniformity in the vertical direction have implications in the transport of solutes between W_{III} phases during the extractive purification of proteins or removal of heavy metals and pollutants from wastewater, or the deposition of BμEs onto hydrophilic vs. hydrophobic surfaces as thin coatings.

Keywords: bicontinuous microemulsions, liquid-liquid extraction, small-angle neutron scattering, Winsor-III systems

Introduction

Bicontinuous microemulsions (BμEs) are unique self-assembly systems that consist of nearly-equal portions of water and apolar solvent. Surfactant monolayers of near-zero curvatures separate polar and apolar nanodomains, and constitute high amounts of interfacial area. BμEs are employed for several applications, including drug delivery, nanomaterial templating, blending of immiscible polymers, enhanced oil recovery, electrochemical analysis, and hosting chemical and biochemical reactions, particularly those that involve reactants differing in polarity [1-14]. BμEs also serve as a biomembrane mimetic system, resembling oil-swollen phospholipid bilayers; but, unlike vesicles, micelles and other mimetic systems, they are isotropic, optically clear, and undergo faster lateral and internal dynamics [15, 16].

BμEs serve as the middle phase of Winsor-III (W_{III}) systems, in equilibrium with water and oil excess phases. Such systems, formed by mixing nearly-equal portions of water and oil, have been employed for the extraction of proteins and metals and removal of pollutants from wastewater [17-23]. They are useful systems for hosting chemical or biochemical reactions, to leverage the aqueous and oil excess phases for continuous delivery of reactants and recovery of products due to exchange of water, oil, and their solubilized components between the phases. W_{III} systems possess ultralow interfacial tension at the lower, but not upper, liquid-liquid interface [24]. Given the vast differences in behavior between the top and bottom liquid-liquid interfaces, it is hypothesized that the BμE phase differs in composition, hence behavior, in the vertical direction. Such differences may impact the transport of solutes within the BμE phase and across the liquid-liquid interfaces, and therefore play a role in the performance of W_{III} systems in separations and hosting reactions. Compositional differences may also affect adhesion and

structure of BμEs deposited onto hydrophilic and lipophilic substrates as thin films [25] or impact the structure and therefore quality of nanomaterials and gels formed using BμE-based templating media.

A unique sample environment for small-angle neutron scattering (SANS) was developed which enabled the hypothesis to be tested. A vertical stage (Figure 1) allowed for W_{III} systems to be probed at specified and precise vertical positions by moving the W_{III} sample upward or downward, with the neutron incident beam remaining fixed in position. Two different W_{III} systems were investigated: water/Aerosol-OT (AOT)/CK-2,13/heptane and water/sodium dodecyl sulfate (SDS)/1-pentanol/dodecane. AOT and SDS are anionic surfactants. CK-2,13 is an alkyl ethoxylate (nonionic surfactant), consisting of a central cyclic ketal (1,3-dioxolane) group, to which are attached two alkyl tails with respectively 2 and 13 carbons and one ethoxylate group averaging 5.6 ethoxylate monomeric units[18]. 1-Pentanol serves as a cosurfactant. Both systems were selected because they provide BμE phases with large volume fractions, hence long vertical distances for SANS measurements [15, 18 23]. In addition, the systems have been investigated by the authors for protein purification and as host systems for membrane-associated peptides and proteins [15, 18, 23]. The SDS/pentanol W_{III} system has been employed for extraction of multivalent cations [17].

The properties of the W_{III} BμE phases for the two systems differ significantly. For instance, the SDS/pentanol system requires a 3.4-fold higher salinity (Table 1). The AOT/CK-2,13 binary surfactant mixture is more efficient at forming BμEs compared to SDS, evidenced by lower concentrations for the former two surfactants in the BμE phases (Table 1), As a result, the nanodomains of AOT/CK-2,13 BμEs are larger and the interfacial area per volume is smaller [15,

[18, 23]. The surfactants AOT and CK-2,13 partition strongly and cooperatively to the BμE W_{III} phase; in contrast, although SDS also partitions strongly to BμEs, pentanol partitions between the top and BμE phases, and likely resides within the BμEs' lipophilic nanodomains and surfactant monolayers [15, 18, 23, 26]. The AOT/CK-2,13 system possesses greater interfacial rigidity [15, 18, 23].

A second objective is to evaluate the utility of the vertical stage sample environment in the SANS analysis of soft matter at specified positions, such as near interfaces. Although the focus of this paper is on W_{III} systems, the approach and instrumentation described herein can also be applied to other multiphasic soft matter system, including W_I and W_{II} microemulsion systems and aqueous two-phase systems formed by polymer/polymer and polymer/salt mixtures or micellar systems above the cloud point temperature [27]. For instance, changes in soft matter structure due to the transport of solute across an interface can be investigated, which may lead to a better understanding of the underlying mechanism for interfacial transport.

Experimental

Materials

SDS (> 99% pure) was obtained from Avantor Performance Materials (Center Valley, PA, USA). O-[(2-tridecyl, 2-ethyl-1,3-dioxolan-4-yl) methoxy]–O-methoxy poly(ethylene glycol), or "cyclic ketal" alkyl ethoxylate surfactants, having average ethoxylate monomeric units of 5.6 (CK-2,13-$E_{5.6}$), was synthesized employing a previously published procedure by our group (95% pure) [28]. Aerosol-OT [sodium bis(2-ethylhexyl) sulfosuccinate or AOT; 98% pure] was purchased from Sigma-Aldrich (St Louis, MO, USA). The HPLC-grade solvents heptane, 1-

dodecane, 1-pentanol, and deuterium oxide (D_2O) were obtained from Fisher (Pittsburgh, PA, USA). Deionized water, 18 MΩ x cm of resistivity, was used throughout.

Methods

Preparation of W_{III} systems. W_{III} systems (600 μL) were formed by mixing aqueous protein + salt and organic solvent-based solutions, with the salinity and/or the surfactant concentration being optimized (equally balanced hydrophilicity and lipophilicity, evidenced by aqueous and organic excess phases being nearly equal in volume, Figure 1A), to allow for rapid phase separation (typically within 1-2 minutes) [18]. For the AOT/CK-2,13 system, the aqueous and organic phases consisted of a D_2O (0.89 wt% [0.15 M] NaCl) /H_2O (0.65 wt% [0.12 M] NaCl) 1:1 v/v mixture, and a heptane solution containing 2 wt% AOT and 2 wt% CK-2,13 in heptane, respectively. Using the following definitions to quantify W_{III} composition:

$$\alpha = M_o / (M_w + M_o) \quad (1)$$

$$\gamma = M_s / M_{total} \quad (2)$$

$$\delta_1 = M_{AOT} / M_s \quad (3)$$

where M_i is the mass of component i (o = oil, w = water, s = surfactant), the AOT/CK-2,13 system is described by α=0.38, γ=0.020, and δ_1=0.50. The SDS/pentanol /dodecane systems were formed according to conditions given in a previous publication [17]. Aqueous solution (D_2O/H_2O 31.22:68.78 v/v, containing 2.4 wt% [0.41 M] NaCl, 3.9 wt% [0.14 M] SDS), and oil (1-pentanol/dodecane, 0.2:1.0 v/v) were mixed at a 1.0/1.2 v/v ratio (α=0.48, γ=0.021). W_{III} systems were allowed to equilibrate in 1.5 mL microcentrifuge tubes for 5.5 days and 6.5 days for the AOT/CK-2,13 and SDS/pentanol systems, respectively, prior to being placed in 40 mm tall, 1 mm pathlength cells custom-made by Hellma Analytics (Müllheim, Germany) and analyzed by

SANS, to assure the systems were truly near thermodynamic equilibrium. SANS analysis in the vertical direction was also employed for the AOT/CK-2,13 system after only 4 hr of equilibration, to serve as a control (Electronic Supplementary Information [ESI]). The samples' BμE phases therefore employed a bulk neutron contrast. The use of partially rather than fully deuterated aqueous phases was employed to reduce the extent of multiple coherent scattering, which can perturb the analysis of SANS data [18]. The composition of the BμE phase for the two W_{III} systems is given in Table 1 [15].

SANS. SANS experiments were conducted using the Bio-SANS instrument at Oak Ridge National Laboratory (ORNL), Oak Ridge, TN USA at room temperature (22±1°C) [29]. Two instrument configurations were employed to collect data over the range of scattering vectors, Q ($4\pi\lambda^{-1}\sin\theta$, where 2θ is the scattering angle and λ the neutron wavelength, 6 Å), 0.003 $Å^{-1} < Q <$ 0.35 $Å^{-1}$, which consisted of sample-to-detector distances (SDD) of 2.5 m and 15.3 m. The center of the area detector (1 m x 1 m General Electric (GE)-Reuter Stokes Tube detector, GE Oil and Gas, London, UK) was offset by 400 mm from the beam. The instrument resolution was defined using circular aperture diameters of 40 mm and 2 mm for source and sample, respectively and separated by distances: 3.2 m (for SDD of 2.5m) and 17.4 m (for SDD of 15.3m). The relative wavelength spread $\Delta\lambda/\lambda$ was set to 0.15. The scattering intensity profiles $I(Q)$ versus Q, were obtained by azimuthally averaging the processed 2D images, which were normalized to incident beam monitor counts, and corrected for detector dark current, pixel sensitivity and background.

From previous studies [15, 18], a sample aperture of 2 mm diameter was determined to be optimal for providing sufficient neutron scattered intensity in 5 min exposure. With the sample aperture size decided, the design criteria aimed to achieve a vertical height for the W_{III} BμE (middle) phase so that spatial variation within the BμE phase could be resolved. From these guidelines, a

total height of 40 mm was determined to be optimal for the custom-designed rectangular cells described above. For example, BμE phases for the AOT/CK and SDS/Pentanol W_{III} systems resulted in a vertical height of ~20 mm and ~15 mm, respectively, i.e., ~50% and ~38% of the total height, respectively. To identify the three different phases and two interfaces of the W_{III} system, a custom-designed rectangular cell was mounted on a precision vertical stage; this stage traveled a total distance of 40 mm and the vertical scans were performed in 0.5 mm step size (Figure 4). The vertical profile of the system was obtained by monitoring variations in the neutron transmission intensity as the rectangular cell was vertically translated, so that the beam aligned with the middle of the top phase initially, and then was lowered in 0.5 mm increments downward to the middle of the bottom phase. At each position of the vertical scan, 5 min exposures of SANS data were collected and classified under five different categories- bottom phase only; bottom/middle interface; middle phase only; middle/top interface; and top phase only. Representative SANS data for vertical positions near the two liquid-liquid interfaces, on both sides of the interfaces is given in Figure S1 of the ESM.

SANS data (*I(Q)* vs. *Q*) were reduced using a standard protocol and analyzed by fitting the data with a nonlinear general scattering law based on form and structure factors [*P(Q)* and *S(Q)*, respectively] implemented in the Igor Pro software package [30].

I(Q) vs. *Q* data was fit using the Teubner-Strey (TS) model [31-33]:

$$I(Q) = \frac{1}{a_2 + c_1 Q^2 + c_2 Q^4} + b \qquad (4)$$

where *b* is the incoherent background (subtracted from data via Porod analysis) and a_2, c_1, and c_2 are coefficients employed to calculate the following parameters for bulk contrast:

$$\xi = \frac{1}{\sqrt{\frac{1}{2}\sqrt{\frac{a_2}{c_2}} + \frac{c_1}{4c_2}}} \quad (5)$$

$$d = \frac{2\pi}{\sqrt{\frac{1}{2}\sqrt{\frac{a_2}{c_2}} - \frac{c_1}{4c_2}}} \quad (6)$$

$$f_a = \frac{c_1}{\sqrt{4a_2c_2}} \quad (7)$$

where ξ is the correlation length, d the quasi-periodic repeat distance (i.e., the distance across aqueous plus oil nanochannels), and f_a the amphiphilicity factor. f_a provides a scale of the extent of ordering at the water-oil interfaces within BμEs, with amphiphilicity (degree of order) decreasing as f_a increases, and ranges from +1 (completely disordered interface; inability to form a cohesive monolayer) to -1 (lamellar phase) [33]. $f_a = 0$ refers to the Lifshitz line ($c_1 = 0$), which is typically slightly higher than the wetting-nonwetting transition, near f_a = -0.33 [33]. For f_a > -0.33, μEs wet one of the two excess phases; but, for f_a < -0.33, "good" μEs exist, indicating the μEs form a lens (i.e., a separate phase) [33].

In the Porod regime (large Q), the following equation was employed to determine S/V, the specific surface area per volume [32]:

$$I(Q) = 2\pi(\Delta\rho)^2 \frac{S}{V} Q^{-4} + b \quad (8)$$

The parameter $(\Delta\rho)^2$ refers to the difference in scattering length density squared (i.e., the neutron contrast).

Results and Discussion

SANS data curves for the BμE phases of both W_{III} systems vs. vertical position are given in Figure 2. The presence of a maximum peak position and Q^{-4} dependence (log-log coordinates) for $Q > Q_{max}$ are indicators of BμE formation. The TS model fit the data well (Figure S2), in agreement with our previous research [15, 18, 23]. Values of TS-derived parameters and *S/V* (via Porod analysis) agree with previous reports for the two systems [15, 18, 23].

It is clear that the scattering curves change significantly with vertical position. For both systems, the scattering curves shift to lower Q in the upward direction, but to a greater extent for AOT/CK-2,13. In the upward direction, the scattering curves for AOT/CK-2,13 become less broad, while for SDS/pentanol, the opposite trend occurs. These trends are reflected by changes of TS- and Porod-derived parameters vs. vertical position. For instance, d (~2 π/Q_{max}) increased in the upward direction, although the extent of the increase is much greater for AOT/CK-2,13 (300 Å) compared to SDS/pentanol (12 Å; Figures 3A and B). For the AOT/CK-2,13 system, the increase of d and ξ in the upward direction (but reaching a plateau ~4 mm from the upper liquid-liquid interface), and decrease of *S/V* (which is inversely proportional to ξ [32]) are consistent in trend, and likely reflect the decrease in surfactant concentration in the upward direction (Figures 3A and C) [18, 23, 33, 34]. These results reflect the ultralow interfacial tension reported for the lower liquid-liquid interface of W_{III} systems [24], which would suggest locally higher surfactant concentrations near the bottom of the BμE phase. The latter may serve as a barrier to transport between the bottom and middle phases, perhaps indicative of a different self-assembly structure in this region. To support this hypothesis, we have seen that proteins slowly and inefficiently diffuse across the lower liquid-liquid interface when proteins are added to bottom phase of pre-formed W_{III} systems [35]. (Protein extraction is much more effective when aqueous protein solutions and oil are mixed together, to form a W_{III} system.) A similar phenomenon may occur

for BμEs upon contact with solid surfaces, of relevance to their employment in drug delivery systems, enhanced oil recovery, and paints and coatings.

The slight decrease of f_a in the upward direction just above the lower liquid-liquid interface for the AOT/CK-2,13 system (Figure 3C) and presumed decrease of surfactant concentration in the upward direction are inconsistent trends, since an increase of surfactant concentration increases the extent of ordering of surfactants at the interface of oil and water nanodomains, leading to a decrease of f_a [18, 23, 33]. Perhaps these results reflect the effect of partitioning of CK-2,13 in the vertical direction, noting that the ethoxylate group of CK-2,13 is broad in its distribution [26]. Moreover, the CK-2,13 surfactants with lower ethoxylate groups would partition away from the lower liquid-liquid interface and may enhance the extent of ordering for the surfactant monolayer.

For the SDS/pentanol system, trends differ from those of the AOT/CK-2,13 system and entail smaller changes of magnitude. Although the increase of d with vertical position in the upward direction is consistent in trend with the AOT/CK-2,13 system (presumably due to a decrease of surfactant concentration, as described above), a constant value occurs near the lower liquid-liquid interface (Figure 3B). (ξ and f_a also do not change for lower vertical positions for the SDS/pentanol system; Figure 3D.) The decrease of ξ in the upward direction for SDS/pentanol is opposite of the trend occurring for AOT/CK-2,13. These results may reflect an increasing gradient of the cosurfactant (pentanol) concentration in the upward direction, noting that pentanol is fully soluble in oil (dodecane) and is poorly soluble in water [36], the major component of the top and bottom W_{III} phase, respectively. The increase of f_a and decrease of ξ in the upward direction (Figures 3B and D), trends consistent with an increase of interfacial fluidity [18], may reflect the known enhancement of interfacial fluidity by medium-chain alkanols [37]. SDS/pentanol

BμEs possess more fluid interfaces than the AOT/CK-2,13 BμEs, observed by the high f_a values (Figures 3C and D).

The incoherent background, *b*, is plotted versus vertical position in Figure 4. Although the data contains significant scatter due to the short data collection time (5 min) for the 2.5 m detector distance, the trend for SDS/pentanol, and AOT/CK-2,13 to a lesser extent, is a slight increase of *b* in the upward direction. We interpret this result as reflecting a higher content of oil in the continuous phase of the BμE as one travels toward the upper, BμE-oil, interface. This trend would suggest a slight decrease of the surfactants' hydrophilic-lipophilic balance (HLB) when traveling in the upward direction.

To explore the effect of equilibration time on structural and compositional changes in the vertical direction, the AOT/CK-2,13 system was also investigated via SANS using the vertical stage sample environment for a W_{III} sample equilibrated for 4 h rather than several days as for the samples discussed so far. SANS curves and the TS-derived parameters *d* and ξ changed with vertical position similar in trend to those displayed in Figures 2A and 3A, but to a much lesser extent (Figures S3-S5). For instance, the change of *d* (and ξ) vs. vertical position spanned only 75 Å (5 Å) (Figure S5A) compared to a span of 300 Å (150 Å) observed in Figure 3A. Changes for f_a, *S/V* and *b* in the vertical direction at the shorter equilibration time were minor and within experimental error (Figures S5B and S6). Therefore, equilibration time plays a role in the extent of differences in structure and composition occurring in the vertical direction. The impact of equilibration time on structural gradients in the vertical direction may impact the performance of W_{III} systems for extractions; for instance, the back-extraction step to recover BμE-encapsulated molecules may be strongly affected by the extent of structural change near a liquid-liquid

interface, which would affect interfacial transport. We are planning additional experiments to further explore the time course of ageing of the observed structural gradient.

Conclusions

The middle, BμE, phase of two W_{III} systems that differ in their properties and behavior, were probed in the vertical direction using SANS with a new vertical stage sample environment. Compositional and structural heterogeneity was observed, particularly near the liquid-liquid interfaces. For both W_{III} systems investigated, SANS results suggest the surfactant concentration increased when traveling in the downward direction, a trend consistent with ultralow interfacial tension of the lower liquid-liquid interface of W_{III} systems. In addition, the SANS incoherent background for the two systems slightly increased in the upward direction, a result representing an increase of oil concentration in the upward direction. For the SDS/pentanol system, the observed decrease of ξ and increase of f_a are consistent with an increase of cosurfactant (pentanol) concentration in the upward direction. In addition, there is a time dependence of the extent of vertical structure heterogeneity for W_{III} systems.

At present, it is not understood whether a structural and compositional gradient is a thermodynamic equilibrium feature of the W_{III} middle phase, or whether the slow mobility of molecules leads to a kinetically trapped state. In any case, the observed gradient should be significant for practical applications of BμEs and further research into the physicochemical origin of this soft matter phenomenon is warranted. Additional research is needed to determine if the trends observed for the AOT/CK-2,13 and SDS/pentanol systems occur for other W_{III} systems, and the impact of surfactant type and charge, cosurfactant and oil chain length (which affect interfacial fluidity and rigidity [37]), and salinity on the changes of structure and composition

in the vertical direction. This paper also demonstrates the potential utility of the vertical stage as a new sample environment for SANS, to probe for differences in structure in soft matter systems at the approach of interfaces.

Conflicts of Interest

There are no conflicts to declare.

Acknowledgments

This research was supported by the Laboratory Directed Research and Development program of Oak Ridge National Laboratory (ORNL), grant 6552. The ORNL Center for Structural Molecular Biology (F.W.P. ERKP291) operates the CG-3 Bio-SANS instrument and is supported by the Office of Biological and Environmental Research of the U.S. Department of Energy (DOE). Research at the High Flux Isotope Reactor of ORNL was sponsored by the Scientific User Facilities Division, Office of Basic Energy Sciences, DOE. Ms. Rachel N. Dunlap (ORNL) helped prepare samples for SANS analysis.

Table 1. Composition of the BμE phase (volume fractions) of Winsor-III systems investigated [15]

W_{III} System	***Oil*** [a]	***Water*** [b]	***AOT (or SDS)***	***CK-2,13 (or 1-pentanol)***
AOT/CK-2,13	0.468±0.033	0.501±0.033	0.014±0.001	0.017±0.001
SDS/Pentanol	0.320±0.039	0.494±0.035	0.051±0.005	0.135±0.013

[a] refers to heptane and dodecane for the systems defined by the surfactants AOT and SDS, respectively; [b] 0.12 M and 0.41 M NaCl in H_2O for the AOT/CK-2,13 and SDS/pentanol systems, respectively

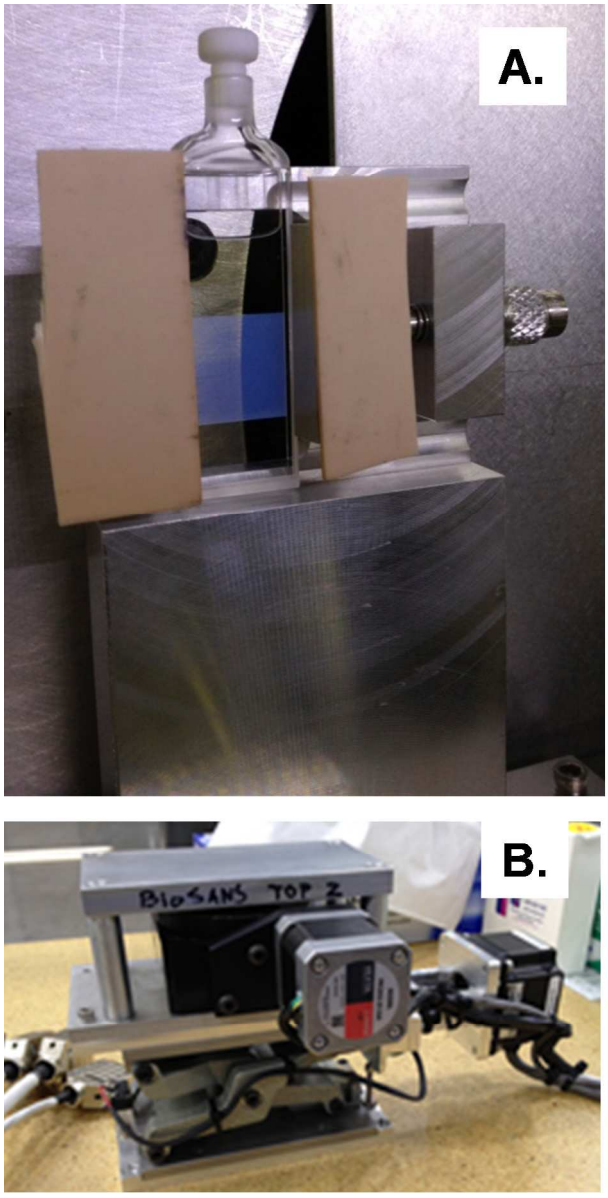

Figure 1. Photographs of vertical stage sample environment, allowing for precise alignment of the sample in the neutron beam through use of a custom-designed rectangular cuvette**. (A)** W_{III} system in the sample holder, which is place on top of a **(B)** motor-controlled vertical stage.

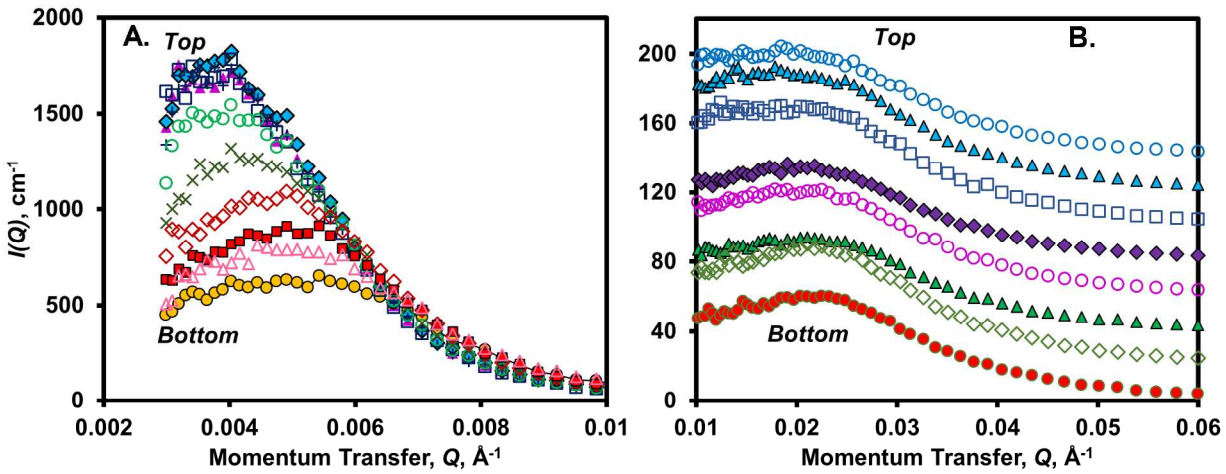

Figure 2. SANS data for the middle, BμE, phase of W_{III} systems formed by (**A)** AOT/CK-2,13 and (**B)** SDS/pentanol. Vertical positions from top to bottom range from 8.5 mm to 28.5 mm by intervals of 2 mm, and 14.0 mm to 26.0 mm by intervals of 2 mm plus 28.5 cm for AOT/CK-2,13 and SDS/pentanol, respectively [for AOT/CK-2,13: (filled circle) 28.5 mm, (unfilled triangle) 26.5 mm, (filled square) 24.5 mm, (unfilled diamond) 22.5 mm, (X) 20.5 mm, (unfilled circle) 18.5 mm, (filled triangle) 16.5 mm, (+) 14.5 mm, (unfilled square) 12.5 mm, (filled diamond) 10.5 mm]. A constant was added to *I(Q)* in Figure B to improve visualization.

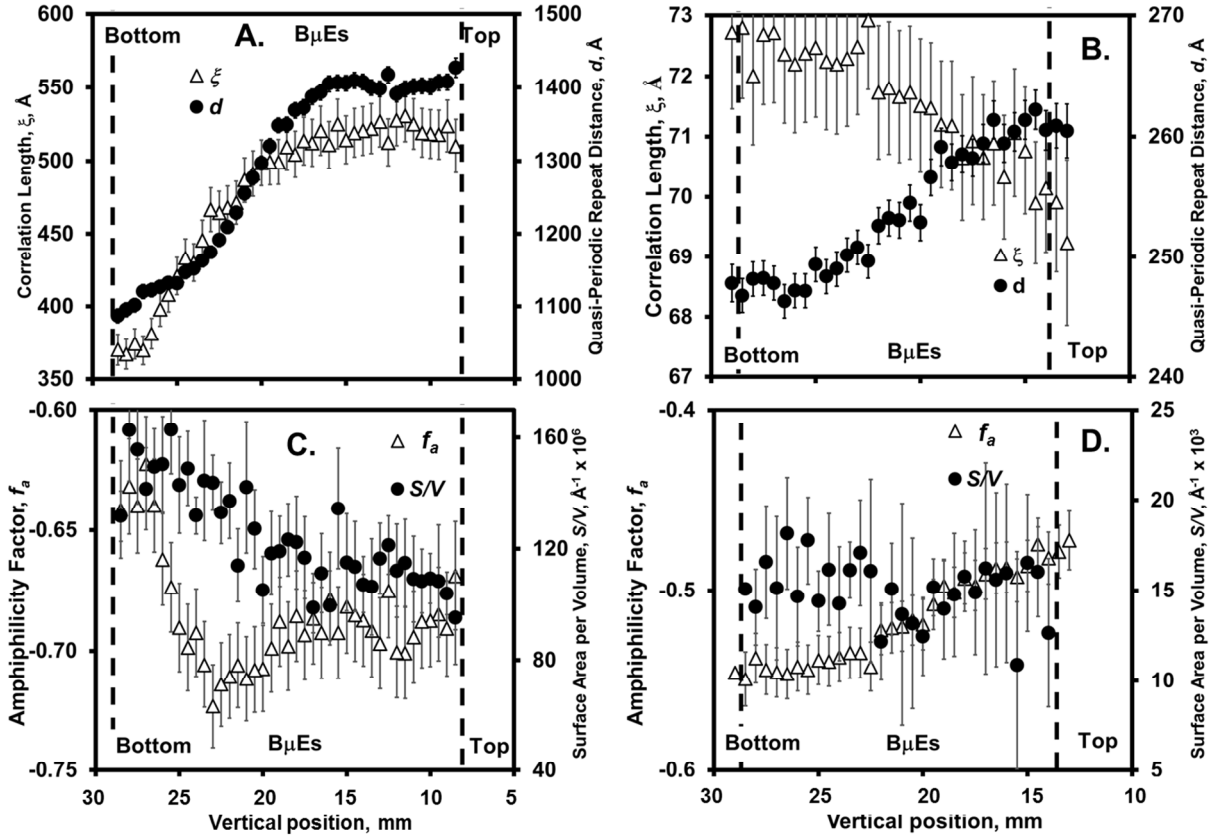

Figure 3. Changes in SANS-derived parameters vs. vertical position in the middle, BμE, phase of W_{III} systems formed by **(A)** and **(C)** AOT/CK-2,13 and **(B)** and **(D)** are SDS/pentanol.

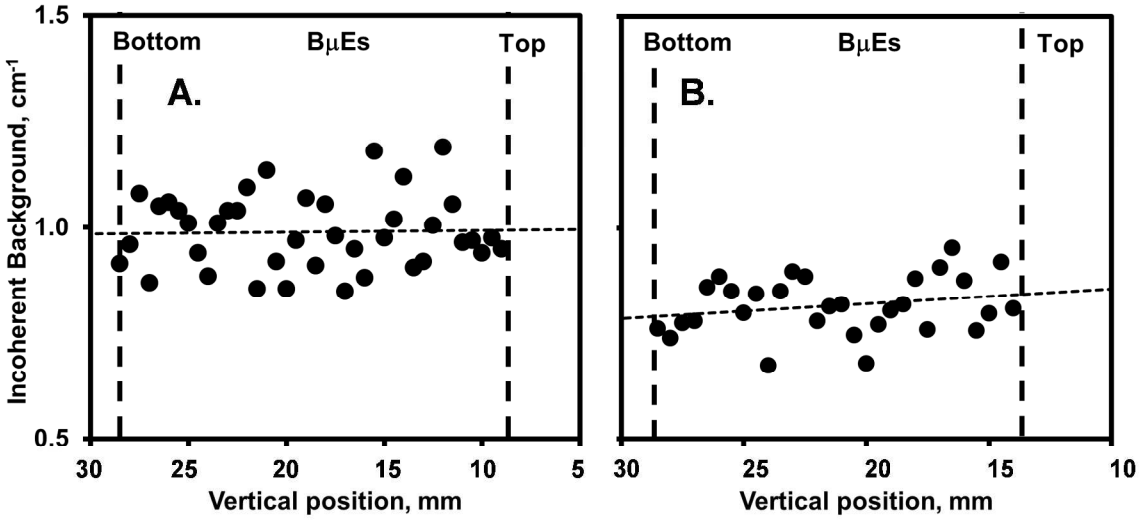

Figure 4. Change of incoherent background vs. vertical position in the middle, BμE, phase of W_{III} systems formed by **(A)** AOT/CK-2,13 and **(B)** SDS/pentanol. Error bars are represented by size of symbols.

References

1. M. Kunitake, E. Kuraya, D. Kato, O. Niwa and T. Nishimi, *Curr. Opin. Colloid Interface Sci.*, 2016, **25**, 13-26.
2. D. Johnson, F. Galiano, S. A. Deowan, J. Hoinkis, A. Figoli and N. Hilal, *J. Membr. Sci.*, 2015, **484**, 35-46.
3. R. Latsuzbaia, E. Negro and G. Koper, *Faraday Discuss.*, 2015, **181**, 37-48.
4. J.-L. Salager, A. M. Forgiarini, R. E. Antón and L. Quintero, *Energy Fuels*, 2012, **26**, 4078-4085.
5. B. H. Jones and T. P. Lodge, *Chem. Mater.*, 2010, **22**, 1279-1281.
6. R. J. Hickey, T. M. Gillard, M. T. Irwin, T. P. Lodge and F. S. Bates, *Soft Matter*, 2016, **12**, 53-66.
7. R. Schwering, D. Ghosh, R. Strey and T. Sottmann, *J. Chem. Eng. Data*, 2015, **60**, 124-136.
8. D. Kipp, O. Wodo, B. Ganapathysubramanian and V. Ganesan, *ACS Macro Lett.*, 2015, **4**, 266-270.
9. A. K. Steudle, B. M. Nestl, B. Hauer and C. Stubenrauch, *Colloids Surf., B*, 2015, **135**, 735-741.
10. X.-Y. Xuan, Y.-L. Cheng and E. Acosta, *Pharmaceutics*, 2012, **4**, 104-129.
11. V. Tchakalova, C. Bailly and W. Fieber, *Flavour Fragrance J.*, 2014, **29**, 67-74.
12. M. Subinya, A. K. Steudle, T. P. Jurkowski and C. Stubenrauch, *Colloids Surf., B*, 2015, **131**, 108-114.
13. L. Deng, M. Taxipalati, P. Sun, F. Que and H. Zhang, *Colloids Surf., B*, 2015, **136**, 859-866.
14. R. M. Hathout and M. Nasr, *Colloids Surf., B*, 2013, **110**, 254-260.
15. D. G. Hayes, R. Ye, R. N. Dunlap, D. B. Anunciado, S. V. Pingali, H. M. O'Neill and V. S. Urban, *Biochim. Biophys. Acta Biomembr.*, 2018, **1860**, 624-632.
16. V. K. Sharma, D. G. Hayes, V. S. Urban, H. M. O'Neill, M. Tyagi and E. Mamatov, *Soft Matter*, 2017, **13**, 4871-4880.
17. J. C. Lopez-Montilla, S. Pandey, D. O. Shah and O. D. Crisalle, *Water Res.*, 2005, **39**, 1907-1913.
18. D. G. Hayes, J. A. Gomez del Rio, R. Ye, V. S. Urban, S. V. Pingali and H. M. O'Neill, *Langmuir*, 2015, **31**, 1901-1910.
19. S. Pondstabodee, J. F. Scamehorn, S. Chavedej and J. H. Harwell, *Sep. Sci. Technol.*, 1998, **33**, 591-609.
20. V. Tricoli, M. Farnesi and C. Nicolella, *AIChE J.*, 2006, **52**, 2767-2773.
21. S. Chavadej, W. Phoochinda, U. Yanatatsaneejit and J. F. Scamehorn, *Sep. Sci. Technol.*, 2004, **39**, 3097-3112.
22. C. S. Vijayalakshmi and E. Gulari, *Sep. Sci. Technol.*, 1992, **27**, 173-198.
23. D. G. Hayes, R. Ye, R. N. Dunlap, M. J. Cuneo, S. V. Pingali, H. M. O'Neill and V. S. Urban, *Colloids Surf., B*, 2017, **160**, 144-153.
24. T. T. L. Nguyen, A. Edelen, B. Neighbors and D. A. Sabatini, *J. Colloid Interface Sci.*, 2010, **348**, 498-504.
25. S. Vargas-Ruiz, O. Soltwedel, S. Micciulla, R. Sreij, A. Feoktystov, R. von Klitzing, T. Hellweg and S. Wellert, *Langmuir*, 2016, **32**, 11928-11938.

26. J. A. Gomez del Rio, D. G. Hayes and V. S. Urban, *J. Colloid Interface Sci.*, 2010, **352**, 424–435
27. B. Y. Zaslavsky, V. N. Uversky and A. Chait, *Biochim. Biophys. Acta Proteins and Proteomics*, 2016, **1864**, 622-644.
28. M. Iyer, D. G. Hayes and J. M. Harris, *Langmuir*, 2001, **17**, 6816-6821.
29. W. T. Heller, V. S. Urban, G. W. Lynn, K. L. Weiss, H. M. O'Neill, S. V. Pingali, S. Qian, K. C. Littrell, Y. B. Melnichenko, M. V. Buchanan, D. L. Selby, G. D. Wignall, P. D. Butler and D. A. Myles, *J. Appl. Crystallogr.*, 2014, **47**, 1238-1246.
30. S. R. Kline, *J. Appl. Crystallogr.*, 2006, **39**, 895-900.
31. M. Teubner and R. Strey, *J. Chem. Phys.*, 1987, **87**, 3195-3200.
32. K. V. Schubert and R. Strey, *J. Chem. Phys.*, 1991, **95**, 8532-8545.
33. K. V. Schubert, R. Strey, S. R. Kline and E. W. Kaler, *J. Chem. Phys.*, 1994, **101**, 5343-5355.
34. S. Maccarrone, D. V. Byelov, T. Auth, J. Allgaier, H. Frielinghaus, G. Gompper and D. Richter, *J. Phys. Chem. B*, 2013, **117**, 5623-5632.
35. J. A. Gomez del Rio and D. G. Hayes, *Biotechnol. Prog.*, 2011, **27**, 1091-1100.
36. M. Góral, B. Wiśniewska-Gocłowska and A. Mączyński, *J. Phys. Chem. Ref. Data*, 2006, **35**, 1391-1414.
37. R. Leung and D. O. Shah, *J. Colloid Interface Sci.*, 1987, **120**, 320-329.

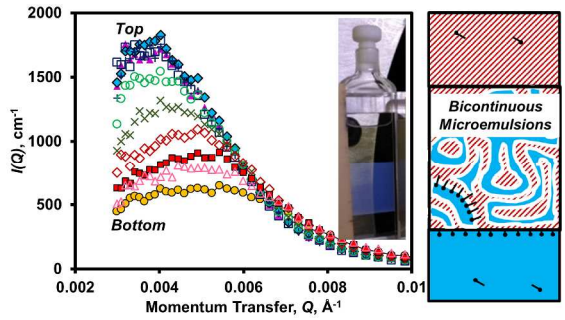

Table of Contents Entry: The structure of bicontinuous microemulsions in Winsor-III systems differs in the vertical direction, as determined using small-angle neutron scattering.